



# Potentiometric Response from Ion-Selective Nanospheres with Voltage-Sensitive Dyes

Xiaojiang Xie, Jingying Zhai, and Eric Bakker\*

Department of Inorganic, Analytical Chemistry, University of Geneva, Quai Ernest-Ansermet 30, CH-1211 Geneva, Switzerland

## S Supporting Information

**ABSTRACT:** Potentiometric sensors require the implementation of conducting wires for signal transduction, but this is impractical for the readout of individual nanoparticles. It is here demonstrated for the first time that the potentiometric response of ion-selective nanospheres can be observed with voltage-sensitive dyes, thereby converting nanoscale electrochemical signals into an optical readout. No reference electrode is needed since the readout is by fluorescence. The results strongly support the potentiometric origin for the fluorescence response. The ion-selective nanospheres exhibit excellent selectivity and respond to ion concentration changes independent of sample pH, providing a new platform of potentiometric nanosensors with optical readout compatible with optical imaging equipment.

Potentiometry is a well-established electrochemical technique that has been extensively studied since the last century.<sup>1,2</sup> Ionophore-based ion-selective electrodes (ISEs) have been widely applied in clinical and environmental monitoring during the past few decades. Ion receptors (ionophores) and ion exchangers are embedded in water immiscible materials, forming a permselective sensing membrane. The phase boundary potential difference ( $\Delta\phi$ ), also referred to as the Nernst potential difference, between the aqueous sample and the sensing membrane is related to the analyte ion activity according to the Nernst equation. For ISEs,  $\Delta\phi$  is measured as an electromotive force with a high input impedance interface at zero current and relative to a reference electrode.

Miniaturization of ISEs holds great promises for a number of cutting-edge applications such as lab-on-a-chip, scanning electrochemical microscopy, and in vivo and intracellular monitoring as well as chemical imaging.<sup>3–8</sup> Microfabrication technologies have entered the field of potentiometry to reduce the size of ISEs down to micrometers and even hundreds of nanometers. Microelectrodes have been designed to monitor the ion activity in cells such as for  $H^+$  and  $Li^+$ .<sup>9,10</sup> However, they do not provide information on spatial distribution from a single, unmoving electrode. Although they have been described in scanning probe microscopy,<sup>11</sup> ISEs are not yet able to image the ion distribution at the submicrometer scale. The intracellular imaging of ions is instead typically performed with fluorescent (bio) molecular probes and nanomaterials.<sup>12–16</sup>

Today, nanoparticles containing ionophore and ion exchangers can be prepared quite readily, but the direct

measurement of  $\Delta\phi$  of individual nanoparticles using electrochemical equipment is not practical. Voltage-sensitive dyes (VSDs) have been previously used to perform membrane potential measurements in organelles and in cells that are too small for microelectrodes.<sup>10,17–20</sup> This work shows that  $\Delta\phi$  can be translated into optical signals by fluorescent VSDs, confirming that  $\Delta\phi$  does not vanish and the chemical principle for ionophore-based ISEs is still valid even at the nanoscale, thereby establishing a new sensing platform.

The nanoparticles were composed of copolymer Pluronic F-127 and lipophilic plasticizer bis(2-ethylhexyl) sebacate (DOS). Driven by van der Waals forces, the lipophilic sensing components, ion-exchanger and ionophore, self-assembled into the lipophilic nanoparticle core.<sup>21–23</sup> The nanospheres produced in this way exhibited an average diameter of ca. 40 nm with excellent thermal stability in aqueous suspension (see Supporting Information for detailed preparation).

In analogy to bulk membrane based ISEs, we presume that an electrical potential difference,  $\Delta\phi$ , is established between the nanosphere interior and the surrounding aqueous phase.<sup>24,25</sup> At electrochemical equilibrium, the electrochemical potential for any target ion,  $I^{z+}$ , must be equal for both phases. One may therefore express  $\Delta\phi$  by eq 1:

$$\Delta\phi = \Delta\phi_I^{0, \text{aq} \rightarrow \text{org}} + \frac{RT}{z_I F} \ln \frac{a_I(\text{aq})}{a_I(\text{org})} \quad (1)$$

where  $\Delta\phi_I^{0, \text{aq} \rightarrow \text{org}}$  is the standard ion transfer potential of  $I^{z+}$ ,  $a_I(\text{aq})$  and  $a_I(\text{org})$  are the activities of the uncomplexed ion in the two phases,  $R$  is the ideal gas constant,  $T$  is the absolute temperature, and  $F$  is Faraday's constant.

In an ideally behaving ISE membrane,  $a_I(\text{org})$  is constant and dictated by the ion-exchange properties and selectivity of the organic phase. In agreement with eq 1,  $\Delta\phi$  increases with increasing ion activity  $a_I$  in the aqueous solution in a Nernstian fashion.

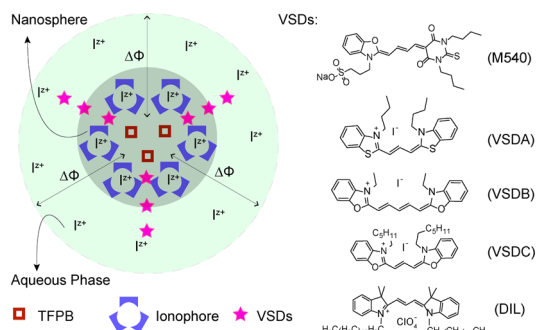
Because of their amphipathic nature, VSDs will distribute in the aqueous phase, the organic nanospheric core, and the interface, with each state contributing to the fluorescence signal (see Scheme 1). The fluorescence of the VSDs used here is sensitive to the polarity of the microenvironment, while the Stark effect is negligible.<sup>20</sup> For instance, 3,3'-dibutylthiacarbocyanine iodide (VSDA) showed a much higher emission intensity in the organic plasticizer DOS than in water (Figure S2, Supporting Information).

Received: August 14, 2014

Published: November 11, 2014



### Scheme 1. Nernstian Potential Difference ( $\Delta\phi$ ) Established between the Aqueous Phase and the Organic Phase of Ion-Selective Nanosphere<sup>a</sup>



<sup>a</sup>Voltage sensitive dyes (VSDs) are able to indicate variations in  $\Delta\phi$  as the  $I^{2+}$  activity in the aqueous phase changes. The free  $I^{2+}$  concentration in the nanosphere remains constant owing to a fixed amount of ion-exchanger (TFPB) and ionophore. For detailed chemical structures, see Figure S1, Supporting Information.

As VSDs are ionic species, their distribution between the organic and aqueous phase is dictated by the electrical potential difference,  $\Delta\phi$ , imposed by eq 1. When  $\Delta\phi$  changes, the VSDs will repartition to adapt to the imposed  $\Delta\phi$  and cause a fluorescence signal change. This repartitioning of VSDs must have negligible influence on  $\Delta\phi$  for them to work as indicators. Indeed, the amount of VSD used here was much smaller than the other components to ensure that VSDs did not themselves influence the value of  $\Delta\phi$ .

VSDs have been explored to make macroscale sensors for  $K^+$ , but the relative signal change, response time, and stability were not yet satisfactory.<sup>26,27</sup> Here,  $K^+$  and  $Ca^{2+}$  were chosen as model ions. Calcium ionophore IV and valinomycin were used as ionophores for  $Ca^{2+}$  and  $K^+$ , respectively. Several different VSDs were screened for nanoscale potentiometry, among which Merocyanine 540 (M540), and VSDA showed the most substantial signal change and were used as the dyes of choice for further experiments. Other VSDs exhibited relatively smaller fluorescence sensitivity but remained functional (Figure S3 in Supporting Information). An optimization of the VSD–ionophore combination is necessary to obtain optimum response. Figure 1 shows the fluorescence response of the potentiometric nanospheres to various analyte concentrations. With increasing ( $K^+$  or  $Ca^{2+}$ ) concentration, the fluorescence intensity for M540 containing system increased (Figures 1a and S4, Supporting Information), while for the VSDA based system, a decrease in emission intensity was observed (Figures 1c and S5, Supporting Information). When used as probes for biological membrane potential, the fluorescence of VSDA is indeed known to decrease upon electric polarization, while for M540, the emission intensity increases.<sup>20,28</sup> This indicated that electric polarization occurred as the analyte concentration increased.<sup>20,28</sup> Nanospheres that contained no ion-exchanger TFPB, however, showed no response to analyte concentration changes, presumably owing to the lack of permselectivity as established by Karpfen and Randles and Bühlmann et al.<sup>29,30</sup>

The incorporation of ionophores improved the selectivity of the nanospheres and lowered the detection limit. Nanospheres based on VSDA (Figures 1d and S5, Supporting Information) exhibited excellent selectivity similar to conventional ISEs and optodes. In the case of M540 (Figures 1b and S4, Supporting Information), the selectivity was inferior to that of conventional

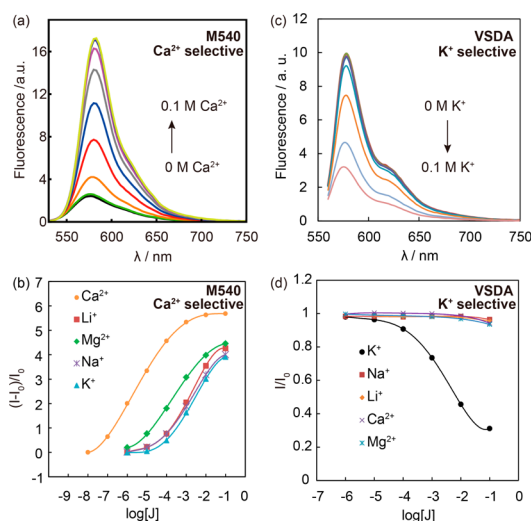


**Figure 1.** (a) Fluorescence spectra of the M540 containing  $Ca^{2+}$ -selective nanospheres with increasing  $CaCl_2$  concentration. (b) Selective response of the M540 containing  $Ca^{2+}$ -selective nanospheres. (c) Fluorescence spectra of the VSDA containing  $K^+$ -selective nanospheres with increasing  $KCl$  concentration. (d) Selective response of the VSDA containing  $K^+$ -selective nanosphere.

ISEs, possibly due to its anionic nature. The detection limit reached 10 nM for  $Ca^{2+}$  and 10  $\mu$ M for  $K^+$ . Fluorescence time traces for the  $Ca^{2+}$ -selective nanospheres are shown in Figure 2a, confirming that the signal is stable, the response time is reasonably rapid ( $t_{95\%}$  of ca. 3 s), and the nanosensor response is fully reversible. Without the use of ionophore, non-discriminative responses to different ions of the same charge were observed instead and the detection limit was much higher (Figure S6, Supporting Information).

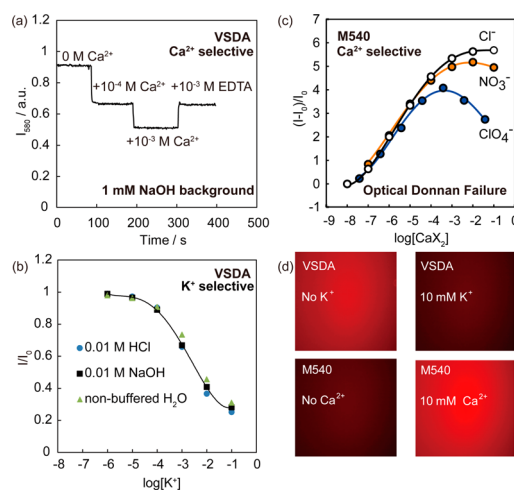


**Figure 2.** (a) Time trace of the fluorescence signal of the VSDA containing  $Ca^{2+}$ -selective nanospheres at 580 nm with gradual addition of  $CaCl_2$  and EDTA as indicated. (b) Response of the VSDA containing  $K^+$ -selective nanospheres in 0.01 M HCl, 0.01 M NaOH, and nonbuffered water. (c) Relative emission intensity change,  $(I - I_0)/I_0$ , as a function of  $CaX_2$  concentration for the M540 containing  $Ca^{2+}$ -selective nanospheres, with various anions X as indicated. (d) Fluorescence microscopic images of the VSDA containing  $K^+$ -selective nanosphere suspension and M540 containing  $Ca^{2+}$ -selective nanosphere suspension without and with 10 mM  $K^+/Ca^{2+}$  as background.

VSDs not only distribute between the bulk phases but are known to also orient themselves at the interface, the extent of which depends on the local electric field and the effective Debye length.<sup>20</sup> Here, VSDA containing K<sup>+</sup>-selective nanospheres were also evaluated in a constant background of either 10 mM HCl or 10 mM NaOH. As shown in Figure 2b, the fluorescence responses under these different conditions were the same compared to those without added electrolyte. This confirms that the optical response is not due to a simple change in Debye length. We assume therefore that the mole fraction of VSDA at the very interface is much smaller than in the two bulk phases, likely owing to the larger thickness of the nanospheres compared to typical bilayer membranes. Moreover, the data demonstrates convincingly that these types of optodes behave largely independent of pH. Ionophore based optodes have suffered from pH cross response that limited their widespread application to a great extent.<sup>24,31</sup> This disadvantage appears to be overcome here by the use of fluorescent potentiometric nanospheres.

For cation-selective ISEs, the upper detection limit is a consequence of coextraction of primary cation and interfering anion from the aqueous phase into the organic phase.<sup>32–35</sup> This effect is loosely known as Donnan (exclusion) failure, although Donnan's experiment did not involve ionophores.<sup>36</sup> More lipophilic anions such as perchlorate are expected to cause more interference compared to less lipophilic anions such as chloride. An optical Donnan failure is observable. As shown in Figure 2c, at high anion concentration, the M540-containing Ca<sup>2+</sup>-selective nanospheres started to show anionic responses in complete analogy to electrochemical devices.<sup>37</sup> Perchlorate and nitrate caused a deviation at lower concentrations and exhibited a lower upper detection limit than chloride in agreement with the Hofmeister sequence.

VSDs are known to be compatible with fluorescence microscopy.<sup>20</sup> Figure 2d shows the fluorescence images of VSDA containing K<sup>+</sup>-selective nanosphere suspensions and M540 containing Ca<sup>2+</sup>-selective nanosphere suspensions. A clear contrast can be observed between nanospheres with and without the addition of Ca<sup>2+</sup> or K<sup>+</sup>.

In the steepest region of the calibration curves, the slope for K<sup>+</sup> is double the value for Ca<sup>2+</sup>, which is again in agreement with the Nernst equation. The sigmoidal shape of the calibration curve is expected on the basis of the optical potential window, beyond which the VSD is fully contained in either phase. Earlier, some other VSDs have been used in reference ion free optodes for K<sup>+</sup> and Cl<sup>−</sup>.<sup>38,39</sup> The sensor response had been simply explained by an extraction equilibrium, but we believe that the physical origin of the distribution process of VSDs is much better described with the interfacial potential difference, especially under experimental conditions where the ion concentrations in the organic phase are effectively not altered by the distribution changes of the VSD.

To summarize, the potentiometric response for neutral ionophore and ion-exchanger containing nanospheres has been investigated using VSDs to translate the Nernst potential difference into fluorescence readout. The results confirmed that even at this small scale, ion-selective electrode theory is still applicable. This work provides a new ion detection platform that is compatible with optical imaging equipment.

## ■ ASSOCIATED CONTENT

### ⑤ Supporting Information

Additional information as noted in the text including the detailed experimental procedures. This material is available free of charge via the Internet at <http://pubs.acs.org>.

## ■ AUTHOR INFORMATION

### Corresponding Author

\*eric.bakker@unige.ch

### Notes

The authors declare no competing financial interest.

## ■ ACKNOWLEDGMENTS

The authors thank the Swiss National Science Foundation (SNF) and the University of Geneva for financial support of this study.

## ■ REFERENCES

- (1) Bakker, E.; Pretsch, E. *Angew. Chem., Int. Ed.* **2007**, *46*, 5660.
- (2) Shim, J. H.; Kim, J.; Cha, G. S.; Nam, H.; White, R. J.; White, H. S.; Brown, R. B. *Anal. Chem.* **2007**, *79*, 3568.
- (3) Denuault, G.; Nagy, G.; Toth, K. In *Scanning Electrochemical Microscopy*, 2 ed.; Bard, A. J., Mirkin, M. V., Eds.; CRC Press: Boca Raton, FL, 2012; p 275.
- (4) Jägerszki, G.; Takács, Á.; Bitter, I.; Gyurcsányi, R. E. *Angew. Chem., Int. Ed.* **2011**, *50*, 1656.
- (5) Lee, C.; Miller, C. J.; Bard, A. J. *Anal. Chem.* **1991**, *63*, 78.
- (6) Rabinowitz, J. D.; Vacchino, J. F.; Beeson, C.; McConnell, H. M. *J. Am. Chem. Soc.* **1998**, *120*, 2464.
- (7) Marzouk, S. A. M.; Buck, R. P.; Dunlap, L. A.; Johnson, T. A.; Cascio, W. E. *Anal. Biochem.* **2002**, *308*, 52.
- (8) Numnuam, A.; Chumbimuni-Torres, K. Y.; Yun Xiang, R. B.; Thavarungkul, P.; Kanatharana, P.; Pretsch, E.; Wang, J.; Bakker, E. *J. Am. Chem. Soc.* **2008**, *130*, 410.
- (9) Ammann, D.; Lanter, F.; Steiner, R. A.; Schulthess, P.; Shijo, Y.; Simon, W. *Anal. Chem.* **1981**, *53*, 2267.
- (10) Thomas, R. C.; Simon, W.; Oehme, M. *Nature* **1975**, *258*, 754.
- (11) Kissa, A.; Nagy, G. *Electrochim. Acta* **2014**, *119*, 169.
- (12) He, Q.; Miller, E. W.; Wong, A. P.; Chang, C. J. *J. Am. Chem. Soc.* **2006**, *128*, 9316.
- (13) Buccella, D.; Horowitz, J. A.; Lippard, S. J. *J. Am. Chem. Soc.* **2011**, *133*, 4101.
- (14) Mank, M.; Griesbeck, O. *Chem. Rev.* **2008**, *108*, 1550.
- (15) Carter, K. P.; Young, A. M.; Palmer, A. E. *Chem. Rev.* **2014**, *114*, 4564.
- (16) Han, J.; Burgess, K. *Chem. Rev.* **2010**, *110*, 2709.
- (17) Reeve, J. E.; Corbett, A. D.; Boczarow, I.; Kaluza, W.; Barford, W.; Bayley, H.; Wilson, T.; Anderson, H. L. *Angew. Chem., Int. Ed.* **2013**, *52*, 9044.
- (18) Yan, P.; Millard, A. C.; Wei, M.; Loew, L. M. *J. Am. Chem. Soc.* **2006**, *128*, 11030.
- (19) Kenet, T.; Bibitchkov, D.; Tsodyks, M.; Grinvald, A.; Arieli, A. *Nature* **2003**, *425*, 954.
- (20) Waggoner, A. S. *Annu. Rev. Biophys. Bioeng.* **1979**, *8*, 47.
- (21) Xie, X.; Mistlberger, G.; Bakker, E. *Anal. Chem.* **2013**, *85*, 9932.
- (22) Xie, X.; Zhai, J.; Bakker, E. *Anal. Chem.* **2014**, *86*, 2853.
- (23) Xie, X.; Bakker, E. *ACS Appl. Mater. Interfaces* **2014**, *6*, 2666.
- (24) Bakker, E.; Buhlmann, P.; Pretsch, E. *Chem. Rev.* **1997**, *97*, 3083.
- (25) Bakker, E.; Buhlmann, P.; Pretsch, E. *Talanta* **2004**, *63*, 3.
- (26) Murkovic, I.; Lobnik, A.; Mohr, G. J.; Wolfbeis, O. S. *Anal. Chim. Acta* **1996**, *334*, 125.
- (27) Wolfbeis, O. S. *Sens. Actuators, B* **1995**, *29*, 140.
- (28) Dragstent, P. R.; Webb, W. W. *Biochemistry* **1978**, *17*, 5228.
- (29) Karpfen, F. M.; Randles, J. E. B. *Trans. Faraday Soc.* **1953**, *49*, 823.

- (30) Bühlmann, P.; Yajima, S.; Tohda, K.; Umezawa, Y. *Electrochim. Acta* **1995**, *40*, 3021.
- (31) Xie, X.; Zhai, J.; Bakker, E. *Anal. Chem.* **2014**, *86*, 8770.
- (32) Boles, J. H.; Buck, R. P. *Anal. Chem.* **1973**, *45*, 2057.
- (33) Buck, R. P.; Cosofret, V. V.; Lindner, E. *Anal. Chim. Acta* **1993**, *282*, 273.
- (34) Buck, R. P.; Toth, K.; Graf, E.; Horvai, G.; Pungor, E. *J. Electroanal. Chem.* **1987**, *223*, 51.
- (35) Yajima, S.; Tohda, K.; Bühlmann, P.; Umezawa, Y. *Anal. Chem.* **1997**, *69*, 1919.
- (36) Donnan, F. G. Z. *Elektrochem. Angew. Phys. Chem.* **1911**, *17*, 572.
- (37) Qin, Y.; Bakker, E. *Anal. Chem.* **2002**, *74*, 3134.
- (38) Huber, C.; Werner, T.; Krause, C.; Wolfbeis, O. S. *Analyst* **1999**, *124*, 1617.
- (39) Krause, C.; Werner, T.; Huber, C.; Wolfbeis, O. S. *Anal. Chem.* **1999**, *71*, 5304.